Acta Cryst. (1972). B28, 936

Complex Cubic A_6B Compounds. II. The Crystal Structure of Mg_6Pd*

BY STEN SAMSON

Arthur Amos Noyes Laboratory of Chemical Physics, California Institute of Technology, Pasadena, California 91109, *U.S.A.*

(*Received* 5 *May* 1971)

Mg_6Pd represents the second of the two structure types so far found for complex A_6B compounds of cubic symmetry containing about 400 atoms each per smallest unit cube, arranged according to space group $F\bar{4}3m$. The first type is represented by Na_6Tl. A complete structure determination has been carried out for Mg_6Pd with the use of packing maps and least-squares refinements employing intensity data of 3233 reflections measured with an automated X-ray diffractometer. The length of the cube edge is $a_o = 20{\cdot}108 \pm 0{\cdot}002$ Å (λ Cu $K\alpha_1 = 1{\cdot}54050$ Å, λ Cu $K\alpha_2 = 1{\cdot}54434$ Å). The calculated density is $\varrho_c = 2{\cdot}905$ g.cm^{-3}, the measured density is $\varrho_m = 2{\cdot}94$ g.cm^{-3} and the final R value is 0·046. This unit cube contains one formula unit of $Mg_{340}Pd_{56}$, and the atoms are distributed among 14 different point sets. Some of the palladium atoms are in substitutional disorder with magnesium, thus giving rise to an extended range of homogeneity. For this reason it seems practical to retain the formula Mg_6Pd as a name for this structure type. The basic building block of the structure consists of a complex of 8 icosahedra, 4 tricapped trigonal prisms and 48 pentagonal prisms. Four such complexes share a Laves–Friauf polyhedron, the center of which is occupied in this case but was empty in Na_6Tl (first type).

Introduction

The existence of the face-centered-cubic phase Mg_6Pd with a_o of the order of 20 Å was established by Ferro (1959) with the application of photomicrography as well as single-crystal and powder X-ray techniques. As was evidenced by careful density measurements and chemical analyses, the phase extends from 56·24 wt% magnesium ($Mg_{5{\cdot}6}Pd$, $\varrho_m = 3{\cdot}011$ g.cm^{-3}, $a_o = 20{\cdot}060$ Å) to 60·75 wt% magnesium ($Mg_{6{\cdot}8}Pd$, $\varrho_m = 2{\cdot}804$ g.cm^{-3}, $a_o = 20{\cdot}182$ Å). Single-crystal photographs indicated the probable space groups $F432$, $Fm3m$, and $F\bar{4}3m$, and attempts to solve the structure by a Patterson projection seemed to have been unsuccessful. The author also states that the unit cell contains between 394 and 398 atoms.

A subsequent paper by Ferro & Rambaldi (1960) reported the existence of a similar compound in the magnesium–platinum system, which, however, appeared to have a narrower range of homogeneity. For the composition Mg_6Pt the authors found $a_o = 20{\cdot}11$ Å and $\varrho_m = 4{\cdot}00$ g.cm^{-3}, which corresponded to 402 atoms per unit cube.

Experimental

Sample preparation

A 10g sample of Mg_6Pd was prepared by melting together 5·78 g of magnesium of 99·8% purity (Matheson Coleman Bell Manufact. Chem.) and 4·22 g of palladium of 99·9% purity (Wildberg Smelting and Refining Co., Los Angeles) in a tantalum thimble which was loaded and hermetically sealed by arc welding under dry argon gas. The tantalum thimble was, in turn, encapsulated hermetically in a stainless-steel cylinder by arc welding under argon gas. All components, including the containers, had been cleaned ultrasonically, then treated with HCl, washed in distilled water, and finally dried under vacuum. The assembly was heated for about two days at 1000°C, frequently agitated, and then cooled to room temperature within a period of about two weeks by gradually reducing the heater current in the resistance furnace.

The bulk of the alloy consisted of several large pieces that appeared to be single crystals. There was no visible attack on the tantalum container by the sample. One alloy fragment was ground to a sphere, and proved by X-ray photographs to be a flawless single crystal.

Unit cell and space group

The crystal used for the subsequent work was a sphere of 0·091 mm radius.

Laue, oscillation, and Weissenberg photographs taken around [001] showed that the structure was face-centered cubic having Laue symmetry $m3m$. Only reflections of the type hkl: $h+k$, $k+l$, $(l+h) = 2n$ were present, indicating that the space group is $F432$, $Fm3m$, or $F\bar{4}3m$.

The length of the cube edge, as determined with the use of a locally designed and built Straumanis-type precision Weissenberg camera of 10 cm diameter, is $a_o = 20{\cdot}108 \pm 0{\cdot}002$ Å. This value was obtained by a Nelson–Riley plot using the 30 highest-order $hk0$ reflections of Cu $K\alpha$ radiation (λ Cu $K\alpha_1 = 1{\cdot}54050$ Å, λ Cu $K\alpha_2 = 1{\cdot}54434$ Å).

* Contribution No. 4249 from Arthur Amos Noyes Laboratory of Chemical Physics. This work was supported by Grant Nos. GP-7984 and GP-17504 from the National Science Foundation.

Table 1. *Observed and calculated structure factors for* Mg_6Pd

Each group of four columns contains, from left to right, indices *l*, observed structure factors, calculated structure factors, and standard deviations. Two dashes indicate that the measured value was given zero weight.

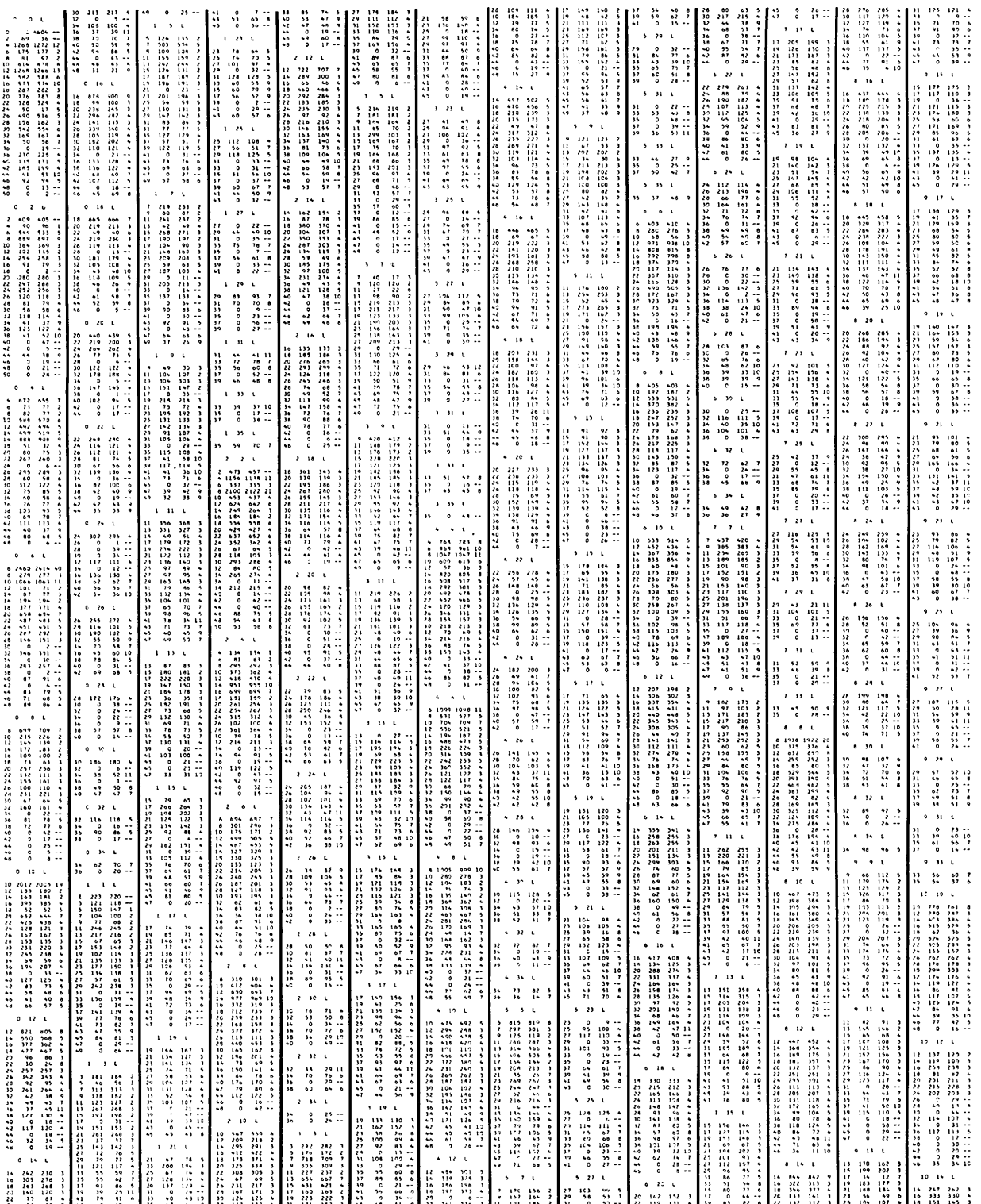

Table 1 (*cont.*)

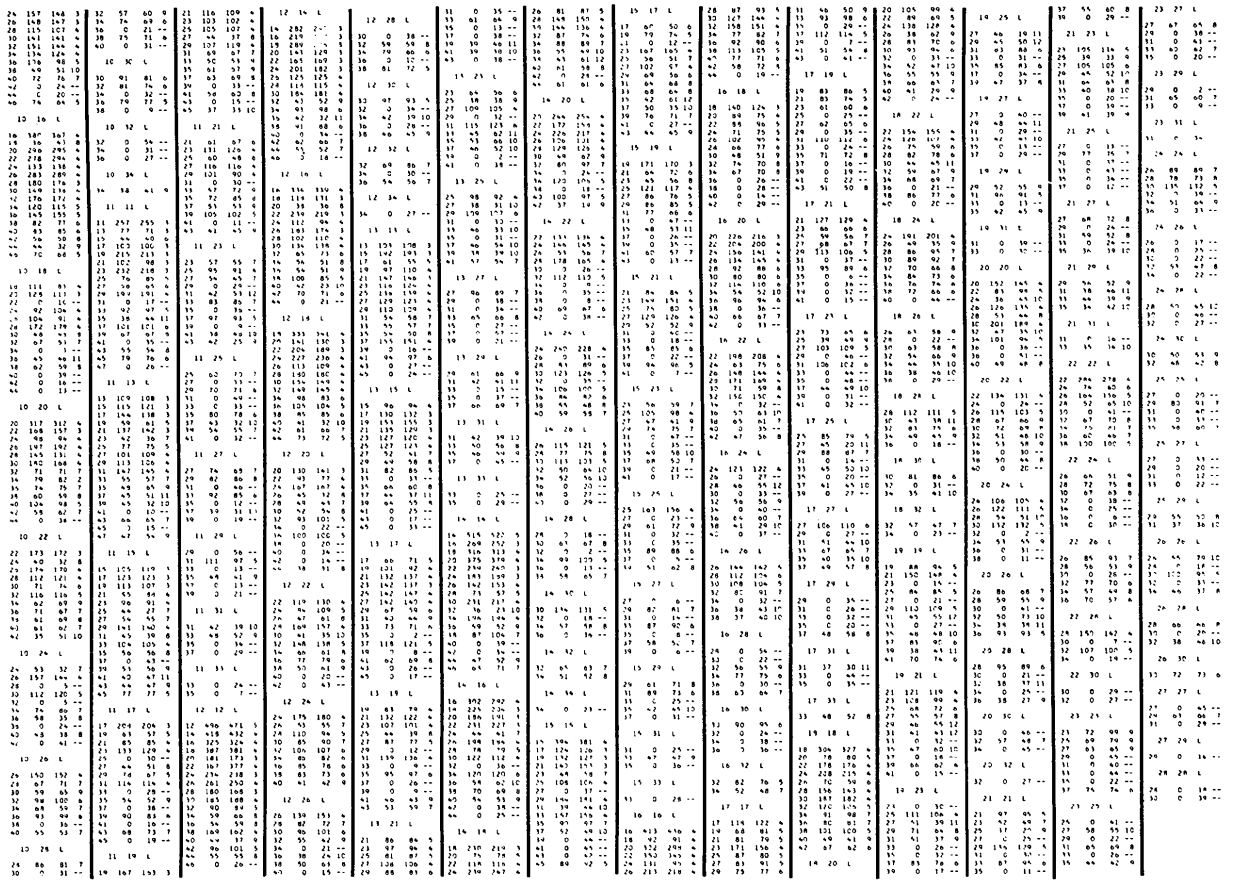

The density measured by weight-loss of small alloy pieces suspended inside a glass bulb in toluene was $\varrho_m = 2{\cdot}94$ g.cm^{-3}. With the sample inside the toluene, the system was evacuated and refilled with air prior to each of two such measurements to remove adsorbed and trapped gas.

Intensity data

The intensities of X-ray reflections were measured and subsequently treated in the same manner as has already been described in the preceding paper on Na_6Tl.

Since in this case the crystal was hard and gave rise to sharp and strong reflections even at high angles, the upper 2θ limit was extended to 124°, and all reflections having intensities less than, or equal to, one standard deviation above background were given zero weight. Spherical absorption-correction factors for $\mu R = 0{\cdot}34$ were applied to the measured intensities. A total of 3233 data was collected (Table 1).

Derivation and refinement of the structure

At the outset, an attempt was made to fit the Na_6Tl type structure into a cube of edge length $a_o = 20{\cdot}108$ Å, assuming 352 magnesium atoms in place of sodium and 56 palladium atoms in place of thallium. The (110) packing map thereby indicated that a considerable number of shortened Mg–Mg bonds would result, thus rendering this model barely acceptable; the unit cell appeared to be somewhat too small to accommodate 408 atoms.

Nevertheless, structure-factor and least-squares calculations were first carried out with the same parameters as those obtained from the Na_6Tl refinement, using the same program, formulae and definitions described in the preceding paper (Samson & Hansen, 1972). The scattering factors, again, were taken from Cromer & Waber (1965) and the anomalous-dispersion correction factors from Cromer (1965).

After three refinement cycles, during which all temperature factors were held constant at $B = 1{\cdot}5$ Å^2, the R value was 0·52, and lack of correlation between the observed and calculated structure factors seemed to rule out the possibility that there was any structural relationship between Na_6Tl and Mg_6Pd. However, the correlation became improved after three more cycles of refinement in which all the temperature factors were included in the matrix, serving as indicators with regard to the distribution of the light (Mg) and heavy atoms

(Pd) over the assumed occupied point sets. The magnitudes of these temperature factors seemed to indicate that the point sets corresponding to Tl(7) and Na(11) (see preceding paper, Samson & Hansen, 1972) had to be omitted, and that those corresponding to Na(10) and Na(12) were occupied in this case by the heavier scatterer palladium [now Pd(11) and Pd(12)]. The temperature factors for Mg(6), Mg(9), Pd(10), and Pd(13) were less than unity, and those of the remaining point sets ranged between 7 and 10.

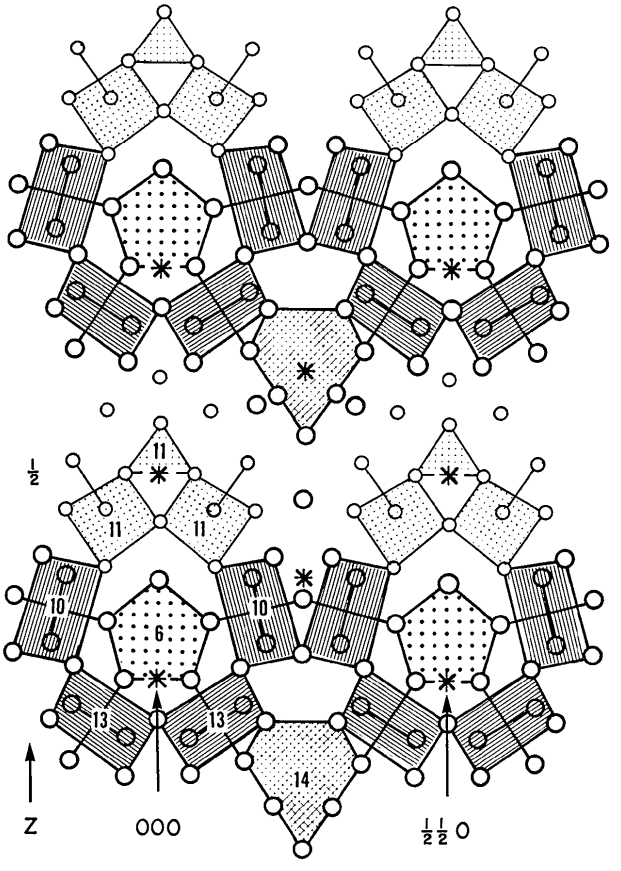

Fig. 1. Packing map of the (110) plane of Mg_6Pd. The asterisks indicate the location of the fourfold inversion centers of space group $F\bar{4}3m$. The polygonal sections marked 10 and 13 represent icosahedra, and those marked 11 represent tricapped trigonal prisms. The section marked 14 represents a Laves–Friauf polyhedron.

The 'most likely atoms' were laid out on the packing map (Fig. 1) to search for a new, reasonable structural motif, keeping in mind that in other noble metal–magnesium compounds such as Mg_3Pd and Mg_3Pt (Na_3As type, Ferro & Rambaldi, 1960), the coordination shell around the noble metal is a tricapped trigonal prism. In the course of this exploration of the packing properties, it became apparent that the point set 24(f) corresponding to Tl(7) had to be reinserted, but this time assuming magnesium atoms and a parameter value x differing by about 1 Å from that of Tl(7). It also became necessary to change some of the other positional parameters to achieve good packing.

At this stage the top icosahedron (marked 7 in Fig. 1 of the preceding paper) was no longer present, and the heavy atoms (palladium) were arranged approximately about a sixfold axis rather than about a fivefold axis (as in Na_6Tl). The packing map almost automatically suggested that each of the two palladium atoms marked 11 in Fig. 1 be surrounded by a tricapped trigonal prism (dotted areas). Thus, the ring of five icosahedra (Fig. 1 in the preceding paper) has been replaced by a ring formed by four icosahedra (marked 10 and 13) and two tricapped trigonal prisms (marked 11 in Fig. 1 of this paper). The only remaining possible space to be filled was the center of the Laves–Friauf polyhedron marked 14 in Fig. 1.

The distribution of atoms just described corresponds to that given in Table 2. It is seen that the point set corresponding to Na(11) is missing in Mg_6Pd.

The 18 positional parameters, the 14 isotropic temperature factors, a secondary extinction parameter, and the scale factor were refined by least-squares calcula-

Table 2. *The refined positional parameters* ($\times 10^5$), *isotropic temperature factors, and occupancies for* Mg_6Pd

The standard deviations are given in parentheses.

Atom no.	Kind	Point set	x	z	B
1	Mg	48(h) xxz, *etc.*	14355 (3)	03398 (5)	1·23 (2) Å^2
2	Mg	48(h) xxz, *etc.*	09395 (3)	27391 (4)	1·24 (2)
3	Mg	48(h) xxz, *etc.*	15097 (3)	52812 (5)	1·76 (3)
4	Mg	48(h) xxz, *etc.*	05655 (3)	76760 (5)	1·48 (2)
5	Mg	48(h) xxz, *etc.*	20016 (3)	90720 (5)	1·95 (3)
6	Mg	24(f) $x00$, *etc.*	10720 (7)		1·12 (3)
7	Mg	24(f) $x00$, *etc.*	38134 (7)		1·27 (3)
8	Mg	24(g) $x\frac{1}{4}\frac{1}{4}$, *etc.*	06482 (7)		1·46 (3)
9	Mg	16(e) xxx, *etc,*	30250 (5)		1·23 (4)
10	Pd	16(e) xxx, *etc.*	16790 (1)		0·994 (6)
11	Pd	16(e) xxx, *etc.*	40653 (1)		0·911 (6)
12	Mg, Pd*	16(e) xxx, *etc.*	66868 (2)		1·72 (2)
13	Pd	16(e) xxx, *etc.*	90038 (1)		0·829 (5)
14	Mg†	4(d) $\frac{1}{4}\frac{1}{4}\frac{1}{4}$, *etc.*			3·05 (21)

* 51·0% Mg; 49·0±0·4% Pd.
† 97±2% Mg.

tions employing a 34×34 matrix. Since the temperature factor of the point set originally assigned to Pd(12) indicated substitutional disorder, the refinement was continued with the inclusion of a population parameter for that point set in the now 35×35 matrix. Finally, a 'partial-occupancy' parameter was introduced for Mg(14) (36×36 matrix).

The refinement converged rapidly, leading to a final R of 0·046 for 2510 reflections with nonzero weight. The final goodness-of-fit was 1·64 and the largest final shift was one-half of its standard deviation (Mg, Pd(12)). The empirical correction factor for secondary extinction [equation (3) of the paper by Larson (1967)] was $g = (7{\cdot}4 \pm 1{\cdot}3) \times 10^{-9}$.

The final positional parameters, the isotropic temperature factors, and the population parameters are given in Table 2. The structure factors are listed in Table 1.

It is seen that the point set 4(d), which is void in Na_6Tl, is in this case occupied by magnesium atoms, but the close coupling between the population parameter and the temperature factor of this set leaves some uncertainty as to the exact degree of occupancy.

Table 2 corresponds to one formula unit of $Mg_{340}Pd_{56}$ per unit cube (or $Mg_{6\cdot07}Pd$). The calculated density (for 396 atoms) is $\varrho_c = 2{\cdot}905$ g.cm^{-3}, which agrees fairly well with the measured value of $\varrho_m = 2{\cdot}94$ g.cm^{-3} and the results obtained by Ferro (1959); see also the Introduction.

It seems appropriate at this time to explain why the above adjustment of the structure model was not done with the aid of Fourier or difference Fourier maps. Such an approach had been tried prior to this work in an attempt to solve the structure of Mg_6Pt, representing a similar cube of $a_o = 20{\cdot}083 \pm 0{\cdot}002$ Å, but was unsuccessful. Parameter and other changes were executed as suggested by one difference map, but the next map invariably suggested changes in the reverse direction, thus leading back toward the starting point. It was first believed that this phenomenon was associated with the nature of the space group $F\bar{4}3m$, which lacks a center of symmetry and has four independent fourfold inversion centers [point sets 4(a), (b), (c), and (d)] each of which may serve as the origin of coordinates. In addition, the structure has several pseudocenters. Since it is now known that neither the Na_6Tl model nor the Mg_6Pd model accounts for the data obtained from the Mg_6Pt crystal, it is believed that the crystal was twinned in a manner that was difficult to detect. In hindsight, the application of difference Fourier or electron density maps to Mg_6Pd might well have been successful.

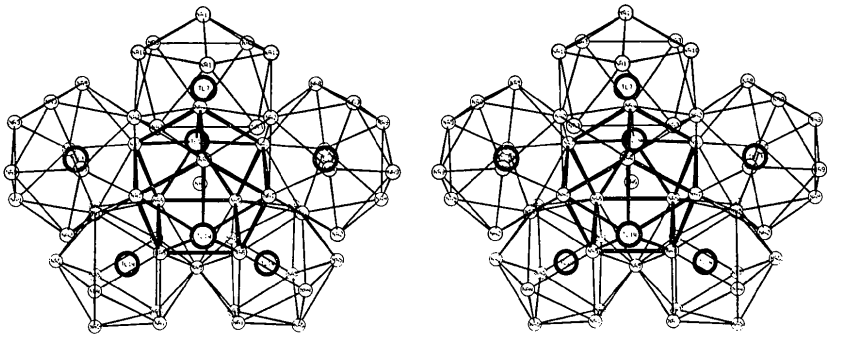

(a)

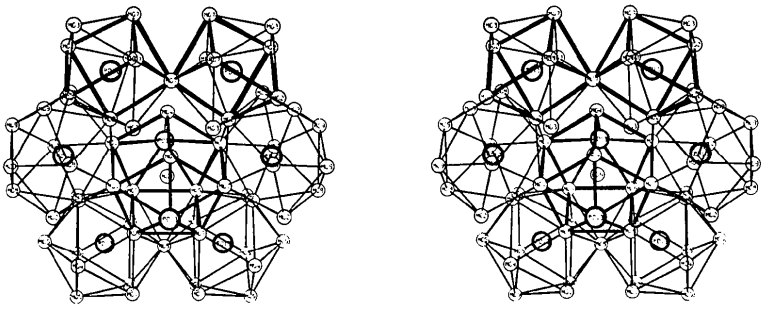

(b)

Fig. 2. (a) A stereo picture of the five icosahedra arranged about a fivefold axis of symmetry representing the basic building block of Na_6Tl. Each large circle represents a thallium atom. (b) The top icosahedron in (a) has been replaced by two tricapped trigonal prisms (dark lines), and there are six palladium atoms (large circles) arranged about a sixfold axis. This is the basic building block of Mg_6Pd. The two models have been drawn to the same scale.

Description of the structure

The structure of Mg_6Pd can be described most conveniently by starting out with the aggregate of five icosahedra arranged about a fivefold axis of symmetry as observed in Na_6Tl and shown in the stereo picture Fig. 2(*a*). This is the same arrangement of polyhedra as that shown in Fig. 2(*a*) of the preceding paper on Na_6Tl. The structural motif of Mg_6Pd is now arrived at by replacing the top icosahedron [around Tl(7)] by two tricapped trigonal prisms [around Pd(11)] as shown in the stereo picture Fig. 2(*b*). Comparison of the two structures shows that the thallium atoms in Na_6Tl (large circles) are arranged about fivefold axes of symmetry, whereas the palladium atoms in Mg_6Pd (large circles) are arranged about sixfold axes, the central pentagonal prism (dark lines) being retained.

From here on, the description of the structure follows along the same lines as in the case of Na_6Tl with the sixfold ring in place of the fivefold ring. Thus, six such sixfold rings interpenetrate one another and share icosahedra so as to form an aggregate corresponding to that shown in Fig. 2(*c*) of the preceding paper, but six of the 14 icosahedra are replaced by 12 tricapped trigonal prisms. When each such aggregate is in its place, each trigonal prism is shared between three adjacent aggregates in such a manner that the average number of prisms per aggregate is four.

The unit cell contains four such aggregates arranged about the points 0, 0, 0, *etc.* [point set 4(*a*)], and sharing edges and faces in such a way that the average number of atoms per aggregate is now 94 (instead of 98 as in Na_6Tl). The four aggregates thus account for 376 atoms per unit cube. Sixteen more atoms [16 Mg, Pd(12)] have to be added, one out from the center of each hexagon of a Laves–Friauf polyhedron shared between four 94-atom complexes arranged about a $\bar{4}$ center. With the addition of four more atoms [4Mg(14)], each at the center of a Laves–Friauf polyhedron, the entire complement of 396 atoms in the unit cell is accounted for.

Discussion of Na_6Tl and Mg_6Pd

Whereas in Na_6Tl each of the 56 thallium atoms is surrounded by an icosahedron, only 32 of the 56 palladium atoms in Mg_6Pd have icosahedral coordination (ligancy 12). Of the remaining 24 palladium atoms, 16 are at centers of tricapped trigonal prisms (ligancy 9) and 8 are in substitutional disorder [Mg, Pd(12)].

Tricapped trigonal prisms are also observed in Mg_3Pt and Mg_3Pd (Na_3As type), but in these cases there is one additional magnesium atom at each of the two extended poles, thus giving rise to ligancy 11.

The 56 thallium atoms are distributed among one 24-fold [Tl(7)] and two 16-fold [Tl(13), Tl(14)] point sets, all of which seem to be ordered, whereas the 56 palladium atoms are distributed among four 16-fold sets [Pd(10), Pd(11), Mg, Pd(12), and Pd(13)], one of which represents substitutional disorder and contains approximately equal proportions of Pd and Mg. It is interesting to see that in the present case this disorder results in the same number of heavy atoms as are observed in Na_6Tl. In view of the considerable range of homogeneity observed for Mg_6Pd (see Introduction), this coincidence of numbers must be accidental.

According to Ferro (1959), the number of palladium atoms per unit cube ranges, at least, from 51 to 60, which may imply that the 16-fold point set [Mg, Pd(12)] could incorporate between 3 and 12 palladium atoms. This point set does not take part in forming the atom complex shown in Fig. 2(*b*), but fills in part of the cavity that is created when each such complex is in its place. Thus, it seems reasonable to assume that Mg, Pd(12) (Table 2) acts as a buffer throughout the entire homogeneity range.

Similarly, the point set 4(*d*) may act as a second buffer by assuming partial occupancy of magnesium (in the case of Mg_6Pd) or sodium (in the case of Na_6Tl), when the compositions of the alloys are varied. Also, this set, corresponding to Mg(14)] [or void (15) in Na_6Tl] does not take part in forming the complexes shown in Fig. 2; instead, it 'fills in' the Laves–Friauf polyhedron, which in the case of Mg_6Pd was found to be occupied and in the case of Na_6Tl proved to be empty (or almost empty).

The difference in the total number of atoms per unit cell in Na_6Tl and Mg_6Pd is caused, in part, by the difference in the number of atoms per complex shown in Fig. 2. The 16-fold point set corresponding to Na(11) is missing in Mg_6Pd, but the fourfold set filling the Laves–Friauf polyhedron which is occupied in Mg_6Pd is empty (or almost empty) in Na_6Tl, thus resulting in a difference of $16-4=12$ atoms in the unit cell contents (408 atoms in Na_6Tl *vs.* 396 atoms in Mg_6Pd).

The differences in the geometrical nature of the two complexes shown in Fig. 2 are also reflected in significant differences in some of the positional parameters, as is seen by comparing Table 2 of this paper with Table 2 of the preceding paper.

The interatomic distances observed in the two compounds are listed in Table 3, with appropriate references to the figures displaying the corresponding polyhedra. Most of these polyhedra are shown in Fig. 3.

A comparison between the distances listed in Table 3 with those observed in other intermetallic compounds containing magnesium [$Mg_3Cr_2Al_{18}$ (Samson, 1958), β-Mg_2Al_3 (Samson, 1965), ε-$Mg_{23}Al_{30}$ (Samson & Gordon, 1968)] shows that many of the Mg–Mg bonds are relatively short; see also in the following section.

Other complex cubic A_6B compounds

Dr Lars Edshammar (University of Stockholm) reported, during his recent visit to this laboratory, that the compounds, Mg_6Rh and Mg_6Ir, form cubes of a size comparable to that of Mg_6Pd, but that the structures had not yet been solved.

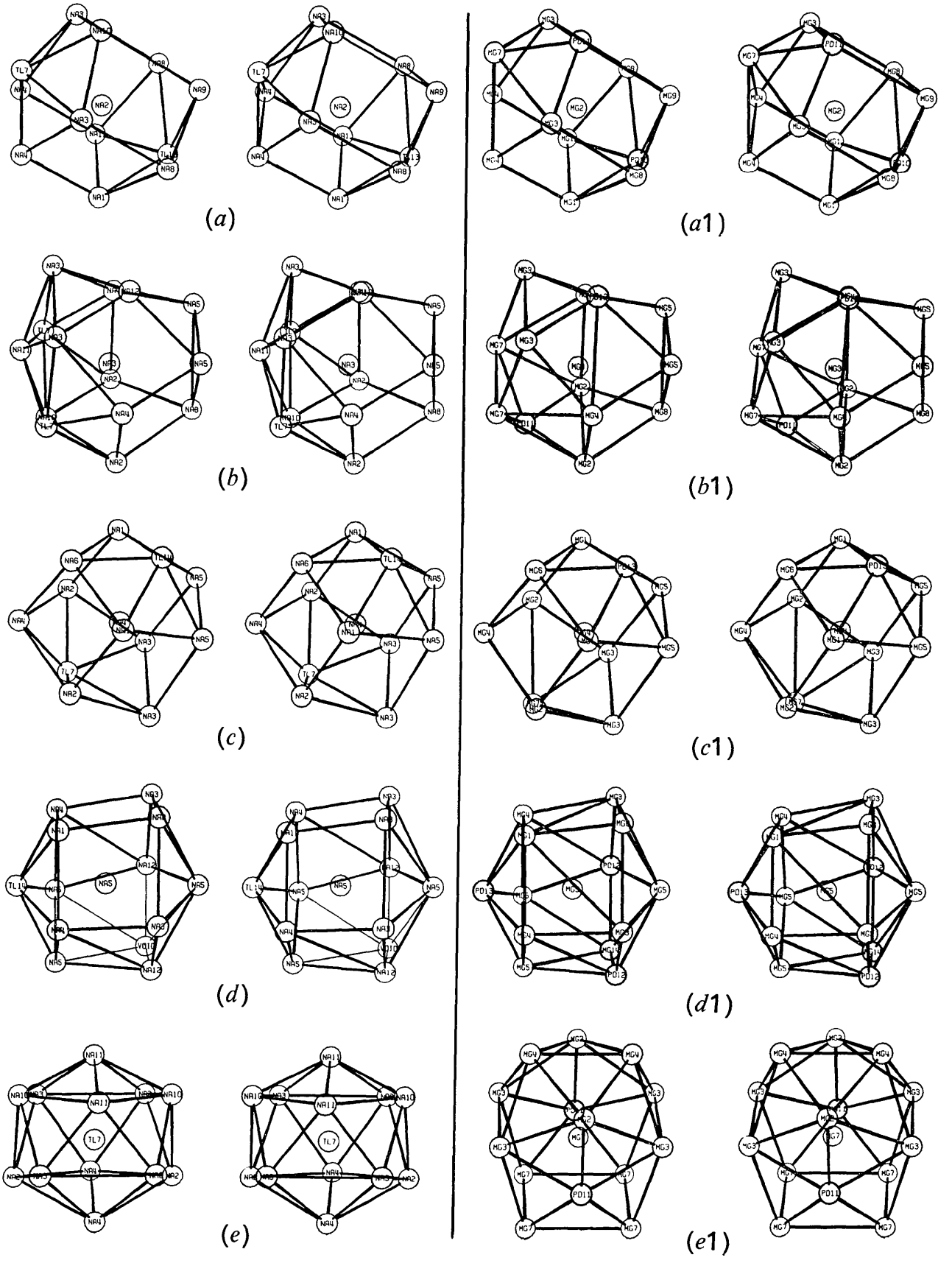
(a)
(a1)
(b)
(b1)
(c)
(c1)
(d)
(d1)
(e)
(e1)

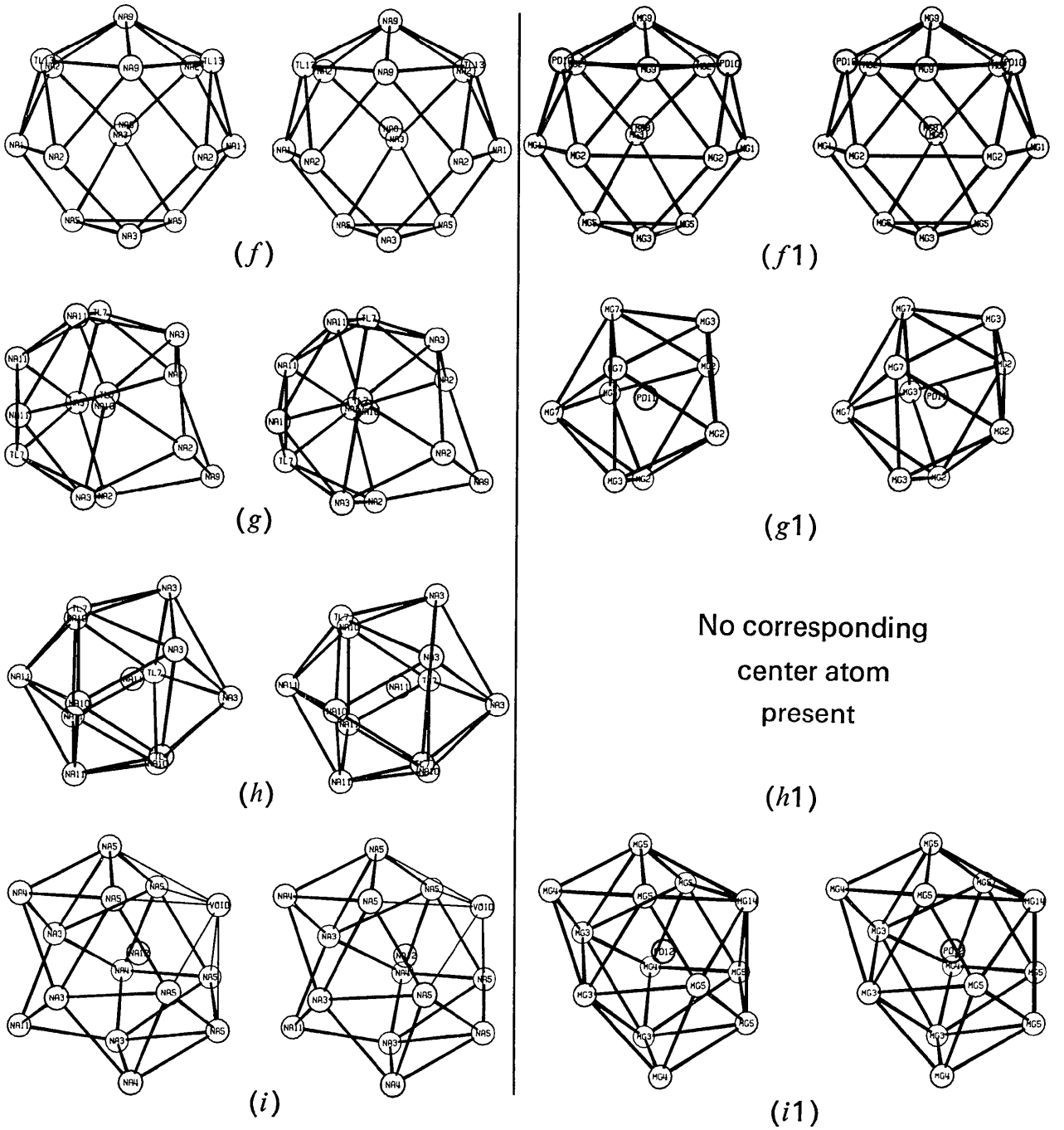

Fig. 3. Each polyhedron displayed in the left column is observed in the structure of Na_6Tl, and the polyhedron shown to the right of it occurs in Mg_6Pd around an analogous point. The point set for Na(11) does not have a counterpart in Mg_6Pd (*h* and *h*1). This is compensated for by rearrangement of the atoms, causing differences in the polyhedra around other center atoms. Thus, (*b*1) has one less ligand [Na(11)] than (*b*), but the polyhedron remains closed because of shifts in Mg(3) and Mg(7). Note that the point corresponding to 'void' in (*d*) is occupied in (*d*1) by Mg(14). Hence, the polyhedron (*d*) is open. The icosahedron (*e*) has been converted to a pentagonal prism (*e*1) which has been deformed to admit two more ligands to the central atom Mg(7), now of the large kind. The most drastic rearrangement is the one leading from (*g*) to (*g*1); Na(9) is not a ligand, and (*g*) is open. Note that Na(11) in (*h*) is displaced toward the center of the triangle formed by 3Tl(7). 'Void' in (*i*) is the unoccupied center of the Laves–Friauf polyhedron, and Na(11) (not a ligand) has no counterpart in (*i*1).

Table 3. *Interatomic distances observed in* Na_6Tl (*left*) *and* Mg_6Pd (*right*)

The figure displaying the polyhedron around each central atom is referred to at the end of each set of distances.

Kind of Atom	Ligancy	Distance (Å)
Na 1	2 Na 1	3.717
	2 Na 2	3.559
	2 Na 4	3.683
	1 Na 5	3.542
	2 Na 6	3.623
	1 Na 8	3.774
	1 Tl 13	3.352
	1 Tl 14	3.522
	12, pentagonal prism + 2, similar to Fig. 3(a)	
Na 2	2 Na 1	3.559
	2 Na 3	3.760
	2 Na 4	3.728
	1 Tl 7	3.472
	2 Na 8	3.928
	1 Na 9	3.767
	1 Na 10	3.568
	1 Tl 13	3.595
	12, Fig. 3(a)	
Na 3	2 Na 2	3.760
	2 Na 3	4.283
	2 Na 4	3.717
	2 Na 5	4.015
	2 Tl 7	3.791
	1 Na 8	4.028
	1 Na 10	3.617
	1 Na 11	3.426
	1 Na 12	3.529
	14, Fig. 3(b)	
Na 4	2 Na 1	3.683
	2 Na 2	3.728
	2 Na 3	3.717
	1 Na 4	3.829
	2 Na 5	3.615
	1 Na 6	3.514
	1 Tl 7	3.169
	1 Tl 14	3.503
	12, Fig. 3(c)	
Na 5	1 Na 1	3.542
	2 Na 3	4.015
	2 Na 4	3.615
	1 Na 5	3.546
	2 Na 5	3.687
	1 Na 8	4.215
	2 Na 12	3.758
	1 Tl 14	3.403
	(1 Void	4.249)
	12, Fig. 3(d)	
Na 6	4 Na 1	3.623
	2 Na 4	3.514
	4 Na 6	3.709
	2 Tl 14	3.378
	12, pentagonal prism + 2, center of Fig. 2(a)	
Tl 7	2 Na 2	3.472
	4 Na 3	3.791
	2 Na 4	3.169
	2 Na 10	3.479
	2 Na 11	3.251
	12, icosahedron, Fig. 3(e)	
Na 8	2 Na 1	3.774
	4 Na 2	3.928
	2 Na 3	4.028
	2 Na 5	4.215
	2 Na 9	3.602
	2 Tl 13	3.701
	14, Fig. 3(f)	
Na 9	3 Na 2	3.767
	3 Na 8	3.602
	3 Na 9	3.598
	3 Tl 13	3.419
	12, icosahedron, not shown	
Na 10	3 Na 2	3.568
	3 Na 3	3.617
	3 Tl 7	3.479
	3 Na 11	3.526
	(1 Na 9	4.717)
	12, Fig. 3(g)	
Na 11	3 Na 3	3.426
	3 Tl 7	3.251
	3 Na 10	3.526
	3 Na 11	3.791
	12, icosahedron, Fig. 3(h)	
Na 12	3 Na 3	3.529
	(3 Na 4	4.613)
	6 Na 5	3.758
	(1 Na 11	4.889)
	(1 Void 15	3.249)
	9, Fig. 3(i)	
Tl 13	3 Na 1	3.352
	3 Na 2	3.595
	3 Na 8	3.701
	3 Na 9	3.419
	12, icosahedron, Fig. 2(a)	
Tl 14	3 Na 1	3.522
	3 Na 4	3.503
	3 Na 5	3.403
	3 Na 6	3.378
	12, icosahedron, Fig. 2(a)	
Void 15	12 Na 5	4.249
	4 Na 12	3.249
	16, Laves-Friauf polyhedron, not shown	

Kind of Atom	Ligancy	Distance (Å)
Mg 1	2 Mg 1	3.116
	2 Mg 2	3.053
	2 Mg 4	3.093
	1 Mg 5	3.015
	2 Mg 6	3.055
	1 Mg 8	3.090
	1 Pd 10	2.781
	1 Pd 13	2.962
	12, pentagonal prism + 2, similar to Fig. 3(a1)	
Mg 2	2 Mg 1	3.053
	(2 Mg 2	3.758)
	2 Mg 3	3.102
	2 Mg 4	3.228
	1 Mg 7	3.436
	2 Mg 8	3.228
	1 Mg 9	3.000
	1 Pd 10	2.994
	1 Pd 11	2.667
	12, Fig. 3(a1)	
Mg 3	2 Mg 2	3.102
	2 Mg 3	3.494
	2 Mg 4	3.071
	2 Mg 5	3.410
	2 Mg 7	3.156
	1 Mg 8	3.380
	1 Pd 11	2.941
	1(Pd, Mg)12	2.871
	13, Fig. 3(b1)	
Mg 4	2 Mg 1	3.093
	2 Mg 2	3.228
	2 Mg 3	3.071
	1 Mg 4	3.216
	2 Mg 5	3.048
	1 Mg 6	2.987
	1 Mg 7	3.399
	1 Pd 13	2.938
	12, Fig. 3(c1)	
Mg 5	1 Mg 1	3.015
	2 Mg 3	3.410
	2 Mg 4	3.048
	1 Mg 5	2.835
	2 Mg 5	3.053
	1 Mg 8	3.472
	2(Pd, Mg) 12	3 112
	1 Pd 13	2.862
	1 Mg 14	3.464
	13, Fig. 3(d1)	
Mg 6	4 Mg 1	3.055
	2 Mg 4	2.987
	4 Mg 6	3.048
	2 Pd 13	2.837
	12, pentagonal prism + 2, center of Fig. 2(b)	
Mg 7	2 Mg 2	3.436
	4 Mg 3	3.156
	2 Mg 4	3.399
	4 Mg 7	3.374
	2 Pd 11	2.706
	14, Fig. 3(e1)	
Mg 8	2 Mg 1	3.090
	4 Mg 2	3.228
	2 Mg 3	3.380
	2 Mg 5	3.472
	2 Mg 9	3.057
	2 Pd 10	3.122
	14, Fig. 3(f1)	
Mg 9	3 Mg 2	3.000
	3 Mg 8	3.057
	3 Mg 9	2.986
	3 Pd 10	2.834
	12, icosahedron, not shown	
Pd 10	3 Mg 1	2.781
	3 Mg 2	2.994
	3 Mg 8	3.122
	3 Mg 9	2.834
	12, icosahedron, Fig. 2(b)	
Pd 11	3 Mg 2	2.667
	3 Mg 3	2.941
	3 Mg 7	2.706
	9, tricapped trigonal prism, Fig. 3(g1)	
(Pd, Mg) 12	3 Mg 3	2.871
	(3 Mg 4	3.758)
	6 Mg 5	3.112
	1 Mg 14	2.832
	10, Fig. 3(i1)	
Pd 13	3 Mg 1	2.962
	3 Mg 4	2.938
	3 Mg 5	2.862
	3 Mg 6	2.837
	12, icosahedron, Fig. 2(b)	
Mg 14	12 Mg 5	3.464
	4(Pd, Mg)12	2, 832
	16, Laves-Friauf polyhedron, not shown	

While the present paper was being prepared, Dr Edshammar sent the author the structural parameters he had obtained from his study of crystals of Mg_6Rh ($a_o = 20{\cdot}1$ Å). He also stated that these parameters did not explain the intensity data his colleague had collected from crystals of Mg_6Pd, and that the latter structure had not yet been solved.

Comparison of his parameters with those obtained here show that Mg_6Rh is isostructural with Na_6Tl. All rhodium atoms are in place of thallium and all magnesium atoms in place of sodium, the Laves–Friauf polyhedron, again, being empty.

Since the noble metals have metallic radii differing by no more than about 2%, the lack of isostructural behavior of Mg_6Rh and Mg_6Pd is surprising, especially since rhodium and palladium are adjacent to each other in the periodic table of the elements. Also, the increased number of magnesium atoms (352 in Mg_6Rh as compared to 340 in Mg_6Pd) results in Mg–Mg bonds that are still shorter than those observed here (see also the Refinement section).

It seems at this stage impossible to predict the type of structure that might be represented by Mg_6Ir and Mg_6Pt or possibly by Mg_6Ru and Mg_6Os (if these two also exist). Each of these will have to be investigated separately with the use of single-crystal data. As stated in the Refinement section, the crystal of Mg_6Pt ($a_o = 20{\cdot}083$ Å) investigated here is still believed to be twinned, but the possibility of the existence of a third and a fourth structure type will, as yet, have to be taken into account.

An important lesson to be learned from the present experience is that one should not draw conclusions from visual inspection of powder photographs as to whether or not intermetallic compounds are isostructural. Unfortunately, this has been done quite frequently in the past and is sometimes still practised today.

I am very thankful to Mr Benes Trus and Mrs Jean Westphal for having provided valuable help with computing problems. I also thank my wife, Mrs Lalli Samson, for having prepared the stereo pictures (Figs. 2 and 3). I am grateful for Mr Anthony Wong's successful efforts to prepare the single crystals.

References

CROMER, D. T. (1965). *Acta Cryst.* **18**, 17.
CROMER, D. T. & WABER, J. T. (1965). *Acta Cryst.* **18**, 104.
FERRO, R. (1959). *J. Less-Common Metals*, **1**, 424.
FERRO, R. & RAMBALDI, G. (1960). *J. Less-Common Metals*, **2**, 383.
LARSON, A. C. (1967). *Acta Cryst.* **23**, 664.
SAMSON, S. (1958). *Acta Cryst.* **11**, 851.
SAMSON, S. (1965). *Acta Cryst.* **19**, 401.
SAMSON, S. & GORDON, E. K. (1968). *Acta Cryst.* B**24**, 1004.
SAMSON, S. & HANSEN, A. (1972). B**28**, 930.

Acta Cryst. (1972). B**28**, 945

The Crystal Structures of 2,4,6-Trichlorobenzonitrile and 2,4,6-Tribromobenzonitrile

BY VIRGINIA B. CARTER AND DOYLE BRITTON

Department of Chemistry, University of Minnesota, Minneapolis, Minnesota 55455, *U.S.A.*

(*Received* 11 *June* 1971)

2,4,6-Trichlorobenzonitrile crystallizes in the monoclinic space group $P2_1/c$ with $a = 3{\cdot}97$ (1), $b = 16{\cdot}06$ (3), $c = 12{\cdot}84$ (2) Å, and $\beta = 91{\cdot}0$ (3)°. 2,4,6-Tribromobenzonitrile crystallizes in the monoclinic space group $P2_1/m$ with $a = 8{\cdot}82$ (2), $b = 10{\cdot}34$ (2), $c = 4{\cdot}89$ (1) Å, and $\beta = 95{\cdot}8$ (2)°. The structures of both compounds were determined from three-dimensional film data and were refined to conventional R values of 0·134 and 0·089, respectively. Neither molecular structure contains any unusual features. The packing of the molecules in the crystals is dominated by weak Lewis acid–base interactions, CN···X, between the cyanide groups and *ortho* halogen atoms in a manner reminiscent of the dimerization of carboxylic acids. In the chloro compound these interactions lead to dimers, with CN···Cl distances of 3·22 Å. In the bromo compound these interactions lead to infinite chain-like polymers, with CN···Br distances of 3·06 Å.

Introduction

Short intermolecular N···X distances are well known in the cyanogen halides (ClCN, Heiart & Carpenter, 1956; BrCN, Geller & Schawlow, 1955; ICN, Ketelaar & Zwartsenberg, 1939) and have recently been found in the halocyanoacetylenes (ClCCCN and BrCCCN, Bjorvatten, 1968; ICCCN, Borgen, Hassel & Rømming, 1962). These short distances have been interpreted as indicating donor–acceptor or acid–base interactions between adjacent molecules. A study of *p*-halobenzonitriles and isonitriles, looking for the same phenomenon (*p*-iodobenzonitrile, Schlemper & Britton, 1965; preliminary results quoted in Britton, 1967), has